Journal of Hydrology 572 (2019) 226–242

Contents lists available at ScienceDirect

Journal of Hydrology

journal homepage: www.elsevier.com/locate/jhydrol

Research papers

Aquifer responses to long-term climatic periodicities

Tanja Liesch*, Andreas Wunsch

Division of Hydrogeology, Karlsruhe Institute of Technology, Institute of Applied Geosciences, Kaiserstr. 12, 76131 Karlsruhe, Germany

ARTICLE INFO

This manuscript was handled by Peter K. Kitanidis, Editor-in-Chief, with the assistance of Simon A. Mathias, Associate Editor

Keywords:
Long-term groundwater level time-series
Wavelet analysis
Climate change
Climatic teleconnections

ABSTRACT

Groundwater is an important resource for drinking water supply, and is subject to natural variation as well as climate change effects. It has been shown that long-term natural variations of groundwater levels can often be attributed to climatic oscillations. Long-term groundwater level records are rare, but of special importance for the detection of longer, decadal to multi-decadal periodicities, which are vital for predictions of future development of groundwater levels and the distinction between natural variation and climate change effects. We have examined periodicities of nine groundwater level time-series with records of more than 100 years, as well as possible impacts of climatic teleconnections (NAO, AMO and ENSO) with wavelet analysis. The monitoring wells are located in Germany, Netherlands, UK and Denmark and cover different depths to groundwater, different aquifer types and hydraulic conditions. Our results show that all evaluated monitoring wells exhibit significant relations to long-term climatic periodicities of NAO, AMO and ENSO. Among the wells in phreatic porous aquifers, there is a signal damping, which can be related to the thickness of the unsaturated zone. Further, the damping is higher in the lower permeable aquifers and there is less damping in the karstic aquifers compared to the porous aquifers, in spite of a much thicker unsaturated zone.

1. Introduction

Groundwater is an important source of freshwater worldwide, and more than two billion people depend on groundwater for drinking water supplies (Mackay et al., 2015; Morris et al., 2003). The understanding of groundwater level fluctuations, including periodicities and trends, is therefore of critical importance for water-resource management issues as it helps to predict future variability of groundwater resources. Periodic control on groundwater levels from oscillatory climatic systems thereby offers a potentially valuable source of longer-term forecasting capability (Rust et al., 2018).

Long-term, systematic measurements of groundwater levels provide essential data needed to evaluate changes in the resource over time (Taylor and Alley, 2001). This is especially the case for differentiating between natural long-term periodic variations of groundwater levels caused by climatic influences (teleconnections), which have been described by many authors in recent years (e.g. Hanson et al., 2004, Fleming and Quilty, 2006, Anderson and Emanuel, 2008, Luque-Espinar et al., 2008, Holman et al., 2011, Tremblay et al., 2011, Perez-Valdivia et al., 2012, Kuss and Gurdak, 2014, Dong et al., 2015, Velasco et al., 2017), climate change effects (Smerdon, 2017) and anthropogenic trends (e.g. caused by over-exploitation).

Since climatic oscillations, which influence precipitation distribution in space and time, show multi-annual to multi-decadal periodicities (Enfield et al., 2001; Brönnimann et al., 2007; Dieppois et al., 2013), these periodicities can also be found in hydrologic processes and time-series like streamflow (Ionita, 2009; Niedzielski, 2011; Massei and Fournier, 2012; Markovic and Koch, 2014), drought frequency and severity (Barros et al., 2017) as well as spring discharges (Charlier et al., 2015; Cox et al., 2009; Huo et al., 2016) and groundwater level responses. Moreover, long-term periodicities are of a higher importance regarding groundwater level fluctuations since high-frequency oscillations are often filtered or damped during the propagation of precipitation signals through the unsaturated zone (Corona et al., 2018; Velasco et al., 2017). However, multi-annual to multi-decadal periodicities have traditionally not been considered in many studies, may it be, because statistical assessments of groundwater records often assume variance and autocorrelation are stationary at extra-annual scales (Rust et al., 2018) or records of groundwater are mostly too short to study long-term periodicities.

While there have been quite a few studies of climatic teleconnections on long (> 80–100 years) precipitation and streamflow records (e.g. Dieppois et al., 2013, Kumar and Duffy, 2009, Fendeková et al., 2014, for a progress report see McGregor, 2017), such long-term measurements of groundwater data are rare. Holman et al. (2011) studied periodicity in a 110 year long groundwater level time-series of a

* Corresponding author.
E-mail address: tanja.liesch@kit.edu (T. Liesch).

https://doi.org/10.1016/j.jhydrol.2019.02.060
Received 30 August 2018; Received in revised form 27 February 2019; Accepted 28 February 2019
Available online 02 March 2019
0022-1694/ © 2019 Elsevier B.V. All rights reserved.

monitoring well in the UK, but most studies focus on groundwater time-series with maximum lengths of < 50 years, which limits the study of decadal and multi-decadal periodicities. Moreover, the relatively short lengths may cause problems with respect to quantifying trends, e.g. related to climate change, in the data (Jackson et al., 2015). Chen and Grasby (2009) e.g. state, that given the predominance of 45–60 year climate cycles observed in instrumental records, trend analyses of time series records less than 60 years should be done with caution, since natural long-term fluctuations in groundwater levels could be misinterpreted as trends, caused by climate change or anthropogenic effects. The study of long groundwater level records is thus of special importance for the detection of longer decadal to multi-decadal periodicities. These are vital for predictions of future groundwater level development regarding their importance for drinking water supply, agricultural irrigation and sensitive ecosystems as well as the risk and impact assessment of groundwater extremes such as land subsidence or groundwater flooding.

A recent review of climatic teleconnection signal control on groundwater variability in Europe is given by Rust et al. (2018), as well as a conceptual model based on current research. They also identified several research gaps, among these are improved quantification of spatial groundwater sensitivity to periodic control, and better identification of the hydrogeological controls on signal lagging and damping.

In this study, we examine periodicities of nine groundwater level time-series with records of more than 100 years (from 1915 to 2016), as well as possible impacts of precipitation and climatic teleconnections on groundwater with wavelet analysis. The monitoring wells are located in Germany, Netherlands, UK and Denmark and cover different depths to groundwater (2.5 to about 30 m), different aquifer types (porous and fractured/karstic) and phreatic and confined conditions.

The considered climatic systems are the North Atlantic Oscillation (NAO), the Atlantic Multidecadal Oscillation (AMO) and the El-Niño Southern Oscillation (ENSO). Several studies found correlations between NAO and precipitation in Europe (e.g. Markovic and Koch, 2005, Massei et al., 2007) and via recharge also on groundwater levels (Luque-Espinar et al., 2008). In a synthesis, Rust et al. (2018) state that while in Northern Europe a positive correlation between winter NAO index and precipitation dominates, Southern and Mediterranean Europe reveal a strong negative correlation between winter NAO and precipitation. In the intermediate zone, the correlation is low overall between positive and negative correlation and diminishes eastward or with distance from the coastline (Rust et al. 2018). While some authors doubt an influence of non-NAO like climatic indices on Europe (Chaudhuri et al., 2011, Alexander et al., 2002), Brönnimann et al. (2007) found relations between ENSO and late winter climate in Europe and Mariotti et al. (2002) could show spatially coherent correlation patterns of interannual variability of rainfall and ENSO for central Europe during winter and spring and for western Europe during autumn and spring. Moron and Ward (1998) concluded from reviews and own studies, that ENSO could explain about 15–20 percent of climate variance in Europe. Already in 1994, Fraedrich (1994) reviewed statistical as well as physical research about a possible long distance teleconnection link between ENSO and Europe and concluded that some analyses support an ENSO-Europe connection, though the conjectures are highly speculative. In the last decade, there is an emerging consensus for a robust link between European climate and ENSO events (Ineson and Scaife, 2009), which can be explained with stratospheric variability (Bell et al., 2009; Domeisen et al., 2015; Herceg-Bulić et al., 2017). Ineson and Scaife (2009) stated that the response of European surface climate to the El Niño Signal is large enough to be useful for seasonal forecasting. Tabari and Willems (2018) recently analysed the extreme precipitation events in Europe and could show that the winter North Atlantic Oscillation (NAO) and, to a lesser extent, winter ENSO signal have a controlling influence not only concurrently on European extreme precipitation anomaly in winter, but in a delayed way on the extremes in the following seasons. Several authors could furthermore show a significant influence of AMO on European climate, especially for the summer months (e.g. Sutton and Hodson, 2005, Knight et al., 2006, Pohlmann et al., 2006). Dieppois et al. (2013) found relations between precipitation and temperature in England and France and AMO. Pohlmann et al. (2006) could show that special AMO states lead to the fact that precipitation is enhanced in northern and decreased in southern Europe, and conclude that some useful decadal predictability may exist. Wyatt et al. (2011) state a significant impact of AMO on the climate in Europe, with a low-frequency, quasi-cyclic climate signal of 50–80 years; Sutton and Hodson (2005) speak of a 65–80 years cycle. The latter might explain why AMO has not been included in studies of groundwater level fluctuations in Europe to date, since these are mostly based on shorter records, a problem that Knight et al. (2006) also state for the climate impacts of AMO.

Based on these findings and assuming that the influence of these climate indices on precipitation and temperature, especially regarding long-term periodicities, is propagated to groundwater levels via recharge, we included the NAO, AMO and ENSO indices in our study. As far as we know, this is the first study of aquifer responses to long-term climatic periodicities including AMO and ENSO in Europe.

2. Data and methods

2.1. Groundwater level and climate data

The groundwater level data comprise time-series of nine wells with monthly records of 102 years (from 1915 to 2016) and were selected based on the length and completeness of the water-level records, as well as available data regarding aquifer, depth and drilling profile. The monitoring wells are located in Germany, Netherlands, UK and Denmark (Fig. 1) and cover different depths to groundwater (2.5 to about 30 m), different aquifer types (porous and fractured/karstic) and phreatic and confined conditions. Though a confining layer could be limiting responses to climatic oscillations (depending on the thickness and hydraulic conductivity), two wells with presumptive confining layers have been included in the analyses. One of them (Dalton Home), attributed as having a thin drift cover, has been analysed before by Holman et al. (2011) and was therefore added for comparison. Furthermore, the variability in the groundwater level of confined to semi-confined wells can nevertheless be subject to climate oscillations at land surface, either as a result of the recharge processes at the (unconfined) distance recharge areas of the aquifer, or by damped recharge through semi-permeable layers. The land uses in the wells' surroundings range from light urban fabric over non-irrigated arable land to forest. Details are given in Table 1. The analysed wells are widely free from anthropogenic influences that might complicate the interpretation of climatic teleconnections, with the exception of Copenhagen and Fuhrberg, where pumping activities of water plants in a distance of about 2 km each started from the 1960 on. Data were obtained either from online services or by request from concerned authorities. Data pre-processing included computing monthly means in the case of higher resolutions, the linear interpolation of occasional smaller data gaps up to four months, and a standardisation to a zero mean and unit variance.

Climate data (precipitation and temperature) were mainly obtained from the U.S. NOAA (National Oceanic and Atmospheric Administration) National Environmental Satellite, Data, and Information Service. The GSOM (Global Summary of the Month) dataset consist of 55 climatological variables computed from summary of the day observations of the Global Historical Climatology Network Daily dataset. Precipitation data for the UK climate stations were taken from the UK Met Office, for Germany, climate data partly originates from the Climate Data Center (CDC) of Germany's National Meteorological Service (Deutscher Wetterdienst). For each groundwater monitoring well, the nearest climate station with the same temporal extent (precipitation data available from 1915 to 2016) was chosen (Fig. 1 and Table 1). In some cases though, the resulting distance from

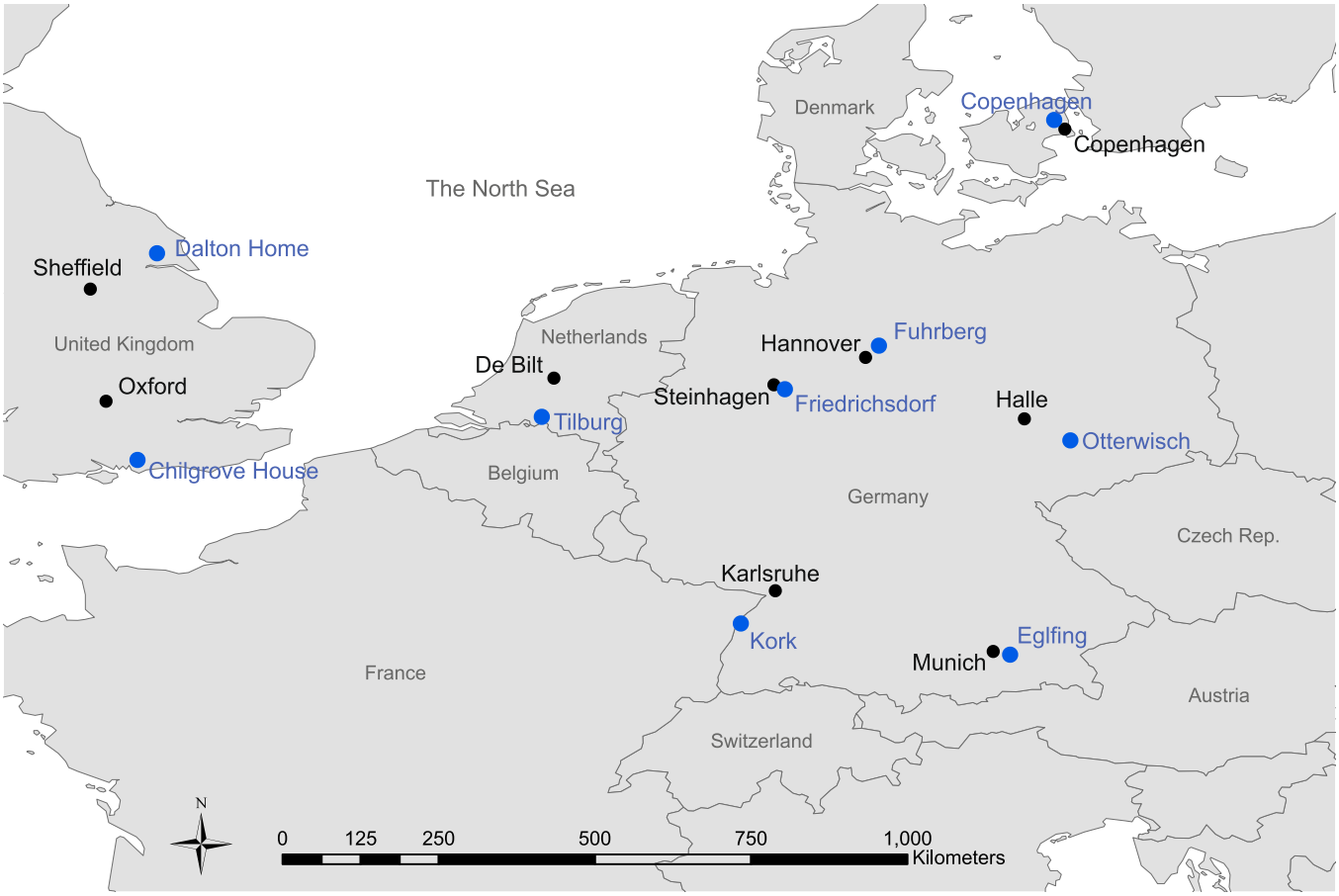

Fig. 1. Location of the nine groundwater monitoring wells (blue) and associated climate stations (black). (For interpretation of the references to colour in this figure legend, the reader is referred to the web version of this article.)

the climate station to the groundwater well is quite far (up to about 100 km in the case of Chilgrove House-Oxford), which probably constitutes some source of error. In the case of Chilgrove House, where a nearer climate station was available (Southampton, in a distance of about 40 km to the well), but not with the same temporal extent, a correlation analysis with was carried out. The correlation for monthly precipitation values of the Oxford and Southampton climate stations resulted in 0.81 (Pearson R, p = 0) for the time of 1915–2000. Taking the relatively high correlation into account, we included the analysis of the precipitation time series of Oxford despite the great distance.

2.2. Climatic indices

2.2.1. North Atlantic Oscillation (NAO)

The North Atlantic Oscillation (NAO) is one of the major modes of variability of the Northern Hemispheres' atmosphere (Hurrell, 1995). It describes the Sea Level Pressure anomalies between the Azores High and the Icelandic Low, and exhibits a principle and secondary periodicity of 8–9 years and of 3–5 years respectively (Hurrell et al., 2003; Hurrell and Deser, 2009). Monthly NAO data, extended back to 1823 by Jones et al. (1997) based on early instrumental data, were obtained from the Climatic Research Unit, University of East Anglia (Jones et al., 1997).

2.2.2. Atlantic Multidecadal Oscillation (AMO)

The AMO is a Sea Surface Temperature (SST) anomaly observed in the North Atlantic with highest intensity in the high latitudes and a low-frequency, quasi-cyclic behaviour of 50–80 years (Wyatt et al., 2011). AMO (unsmoothed, monthly) data were taken from the U.S. NOAA Earth System Research Laboratory (Enfield et al., 2001).

2.2.3. El-Niño/Southern Oscillation (ENSO)

The ENSO is a globally dominating mode of interannual climate variability and affects weather and climate worldwide (Brönnimann et al., 2007). A number of indices are available. We employ monthly data of the NINO3.4 index (SST averages over the area 170–120°W and 5°S–5°N) from the U.S. NOAA Earth System Research Laboratory (Rayner et al., 2003). The often-used Multivariate ENSO Index (MEI) could not be used, since its records only start in 1950. The NINO 3.4 index was chosen, since this area was identified as being the most ENSO-representative (Bamston et al., 1997; Trenberth, 1997).

2.3. Climatic control of groundwater levels

The influence of climate on groundwater levels is given by groundwater recharge signals related to precipitation (P) and evapotranspiration (ET). Evapotranspiration is thereby mainly controlled by temperature (T). The propagation of the recharge signal through the unsaturated zone is quite complex though. In their review, Rust et al. (2018) give a good overview of current research. Main findings are that the unsaturated zone dampens precipitation signals and the damping capacity becomes greater with increased depth and lower hydraulic conductivity, that shorter periodic recharge signals are more sensitive to damping, signals get lagged on their way through the unsaturated zone, driven by the same characteristics as for damping, and the unsaturated zone does not stretch periodic signals but preserves their periodicity (Bloomfield and Marchant, 2013; Dickinson et al., 2014; Gurdak et al., 2007; Holman et al., 2011; Kuss and Gurdak, 2014; Van Loon, 2015). In a recent study, Corona et al. (2018) evaluated the damping depth of transient recharge over a range of periodic boundary conditions, vadose zone geometries and hydraulic parameters, based on

Table 1
Groundwater monitoring wells and climate stations. Well IDs refer to the IDs used by local authorities. Lat/Lon coordinates are given in decimal degrees (WGS84). Depth to groundwater refers to the mean water level of the study period (1915–2016). Land use was taken from CORINE LandCover data (EEA, 2012).

Well name	Well ID	Well location		Geology	Aquifer type	Hydraulic conditions	Average depth to ground-water (m)	Land use	Climate station
		Lon	Lat						
Chilgrove House	SU81/1	0.81 W	50.92 N	Chalk	Fractured/Karstic	Unconfined	28.16	Non-irrigated arable land, broad-leaved forest	Oxford
Copenhagen	155388	12.38 E	55.82 N	Sand with confining clay/silt layer	Porous	Confined	6.67	Industrial or commercial units, discontinuous urban fabric	Copenhagen
Dalton Home	SE94/5	0.53 W	53.90 N	Chalk with thin drift cover	Fractured/Karstic	Unconfined to confined	17.39	Pastures, sport and leisure facilities, non-irrigated arable land	Sheffield
Eglfing	16006	11.75 E	48.12 N	Quarter-nary alluvium	Porous	Unconfined	13.44	Discontinuous urban fabric, non-irrigated arable land, transitional woodland-shrub	Munich
Friedrichsdorf	020104054	8.50 E	51.94 N	Quarter-nary sand and gravel	Porous	Unconfined	3.32	Complex cultivation patterns, mixed forest	Steinhagen
Fuhrberg	400000227	9.86 E	52.57 N	Quarter-nary alluvium	Porous	Unconfined	4.08	Discontinuous urban fabric, non-irrigated arable land, coniferous forest	Hannover
Kork	0115/114-5	7.87 E	48.57 N	Quarter-nary alluvium	Porous	Unconfined	2.50	Discontinuous urban fabric, non-irrigated arable land, complex cultivation patterns	Karlsruhe
Otterwisch	47410003	12.61 E	51.20 N	Quarter-nary alluvium	Porous	Unconfined	2.43	Discontinuous urban fabric, non-irrigated arable land, broad-leaved forest	Halle
Tilburg	B50E0111	5.01 E	51.54 N	Quarter-nary alluvium (coarse to medium sand)	Porous	Unconfined	3.24	Coniferous and mixed forest, moors and heathland, complex cultivation patterns	De Bilt

HYDRUS-1D simulations. They found that mean infiltration flux, period of time varying infiltration, and hydraulic conductivity are statistically significant predictors of damping depth.

Based on these findings we applied univariate wavelet analyses to study periodicities in all analysed time series and cross wavelet analyses between groundwater level time series, precipitation and climatic indices time series to study common periodicities and coherence. Temperature time series were also assessed, but did not show meaningful results concerning long-term periodicities.

Additionally, the average power of the wavelet analyses was evaluated against hydrogeological parameters like depths to water, hydraulic conditions and aquifer type.

2.4. Wavelet analysis

Wavelet analysis is a powerful method that provides an effective approach for non-stationary time series, like hydrologic, atmospheric and other geophysical time series, and has been widely applied in different fields. A review on the applications of wavelet transform in hydrology time series analysis for example has been given by Sang (2013). Wavelet transforms expand time series into time-frequency space and can therefore find localized intermittent periodicities (Grinsted et al., 2004). There are two classes of wavelet transforms, the Continuous Wavelet Transform (CWT) and the Discrete Wavelet Transform (DWT). The DWT is particularly useful for decomposing signals into different frequencies and e.g. applied in noise reduction and data compression, whereas CWT is a common tool for the analysis of localized intermittent periodicities in a time series. When two CWTs are analysed together, a Cross Wavelet Transform (XWT) is constructed, which exposes the common power (continuous wavelet cross-correlation) and relative phase (continuous wavelet coherence, WTC) in time-frequency space (Grinsted et al., 2004). Continuous wavelet cross-correlation provides a time-scale distribution of the correlation between two signals, whereas continuous wavelet coherence provides a qualitative estimator of the temporal evolution of the degree of linearity of the relationship between two signals on a given scale (Labat, 2005). Maraun and Kurths (2004) recommend the use of continuous wavelet coherence (WTC) for the testing of causal relations between two time series, since continuous wavelet cross-correlation can show misleading results, if one of the time series exhibits strong peaks in wavelet power, whereas wavelet coherence overcomes this problem by normalizing the single wavelet power. The WTC, which ranges from zero to one and measures the correlation and phase shift between two time series as a function of frequency, can be interpreted as a correlation coefficient between the two time series.

Detailed theory of wavelet analysis has been extensively elucidated in many works, therefore we refer the reader to relevant literature, like e.g. Foufoula-Georgiou and Kumar (1994), Kumar and Foufoula-Georgiou (1997), Torrence and Compo (1998), or Grinsted et al. (2004) for further details.

In this study, we used CWT and XWT, with a Morlet wavelet, which is a good choice, since it provides a good balance between time and frequency localization (Torrence and Compo, 1998, Grinsted et al., 2004). Monte Carlo methods with a total of 1,000 realizations were used to assess the statistical significance ($p < 0.05$) against red noise backgrounds (first-order autoregressive, AR1), as proposed by Torrence and Compo (1998) and Grinsted et al. (2004) and previously used by several authors (e.g. Holman et al., 2011, Massei et al., 2007).

The wavelet analyses was done with the original monthly data, as applied in similar studies by Holman et al. (2011), Huo et al. (2016) or Luque-Espinar et al. (2008), as well as with deseasonalized data, as suggested by e.g. Kuss and Gurdak (2014). The inclusion of the seasonal cycle allows additional insight, especially regarding the propagation of the recharge signal through the unsaturated zone (lagging and damping of different frequencies), while removing the seasonal cycle prior to the analyses was additionally done to check, whether longer-periodic

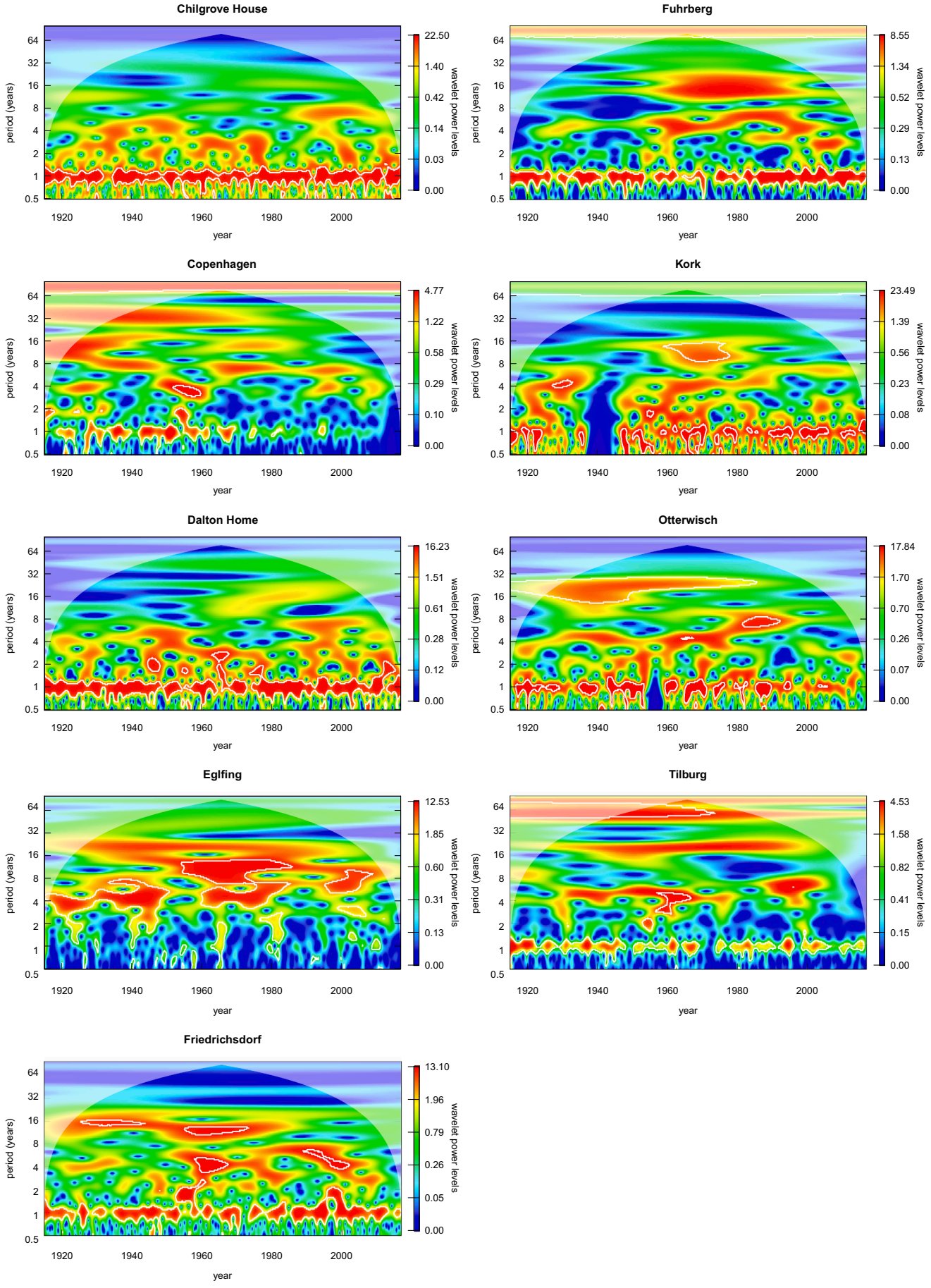

(caption on next page)

Fig. 2. Continuous wavelet power spectra of the nine regarded groundwater wells. Significant local maxima of the average power spectrum with average power and period are given in Table 2.

Table 2
Results of univariate wavelet analyses for the evaluated groundwater wells, precipitation and climate indices: Significant local maxima (global maximum in bold) of the average power spectrum with average power and period.

Groundwater wells						
Well name	Aquifer type	Hydraulic conditions	Depth to groundwater (m)	Period (years)	Average power	p-Value
Chilgrove House	Fractured/Karstic	Unconfined	28.16	0.5	1.182	0.005
				1.0	**10.086**	**< 0.001**
Copenhagen	Porous	Confined	6.67	1.0	0.982	< 0.001
				84.4	**2.838**	**0.012**
Dalton Home	Fractured/Karstic	Unconfined to confined	17.39	**1.0**	**7.730**	**< 0.001**
Eglfing	Porous	Unconfined	13.44	4.6	2.819	< 0.001
				7.2	2.248	0.033
				11.3	**3.957**	**0.008**
Friedrichsdorf	Porous	Unconfined	3.32	**1.0**	**4.147**	**< 0.001**
Fuhrberg	Porous	Unconfined	4.08	**1.0**	**3.659**	**< 0.001**
				84.4	1.994	< 0.001
Kork	Porous	Unconfined	2.50	**1.0**	**5.014**	**< 0.001**
				84.4	0.689	< 0.001
Otterwisch	Porous	Unconfined	2.43	**1.0**	**5.414**	**< 0.001**
				22.6	1.710	0.001
Tilburg	Porous	Unconfined	3.24	1.0	1.472	< 0.001
				57.7	**2.648**	**0.03**
Precipitation						
Climate station				Period (years)	Average power	p-Value
Oxford				**1.0**	**1.631**	**0.019**
				1.9	0.874	0.024
				6.7	0.335	0.026
Copenhagen				**1.0**	**3.264**	**< 0.001**
Sheffield				**1.0**	**1.886**	**< 0.001**
Munich				**1.0**	**7.540**	**< 0.001**
Steinhagen				**1.0**	**1.635**	**0.009**
				4.6	0.614	0.001
				40.8	0.067	0.037
Hannover				**1.0**	**2.541**	**< 0.001**
				4.4	0.475	0.039
Karlsruhe				**1.0**	**1.613**	**0.018**
				13.9	0.167	0.043
Halle				**1.0**	**4.685**	**< 0.001**
				28.8	0.153	0.013
				84.4	0.065	0.034
De Bilt				**1.0**	**2.415**	**< 0.001**
				6.3	0.359	0.036
Climate indices						
Climate index				Period (years)	Average power	p-Value
NAO				**0.5**	**2.725**	**0.037**
				12.6	0.202	0.035
				33.1	0.096	0.028
AMO				1.0	1.386	< 0.001
				57.7	**3.680**	**< 0.001**
				84.4	1.811	0.001
ENSO				0.5	0.882	< 0.001
				1.0	**5.114**	**< 0.001**
				2.5	2.441	0.046

fluctuations are being superimposed by a strong seasonal behaviour. In the following, only the results of the original data are referred to. There were only minor differences in the results after removing the seasonal cycle, especially regarding significance in the univariate wavelet analyses, i.e. some of the longer periods became significant on average, that have not been significant before, while the main results, especially regarding the maxima of the average cross wavelet coherences remained overall unchanged. For completeness, the results of the wavelet analyses with the deseasonalized data are given in the electronic supplementary.

All computations were done in R (R Core Team, 2017), using the WaveletComp package (Roesch and Schmidbauer, 2014).

3. Results and discussion

3.1. Univariate wavelet analyses of groundwater wells, precipitation and climate indices

The univariate wavelet analyses give an overview of significant periodicities of the single time series. The power spectra of the groundwater wells are shown in Fig. 2, the local maxima of the power spectra are given in Table 2. All wells but one show a typical yearly cycle; for six out of nine wells, the 12 months period is the global power maximum. The well without a 12 months periodicity is Eglfing, which is an unconfined well with a rather high depth to groundwater of 13.44 m (Table 1). The maxima of the power spectrum are at about 5, 7 and

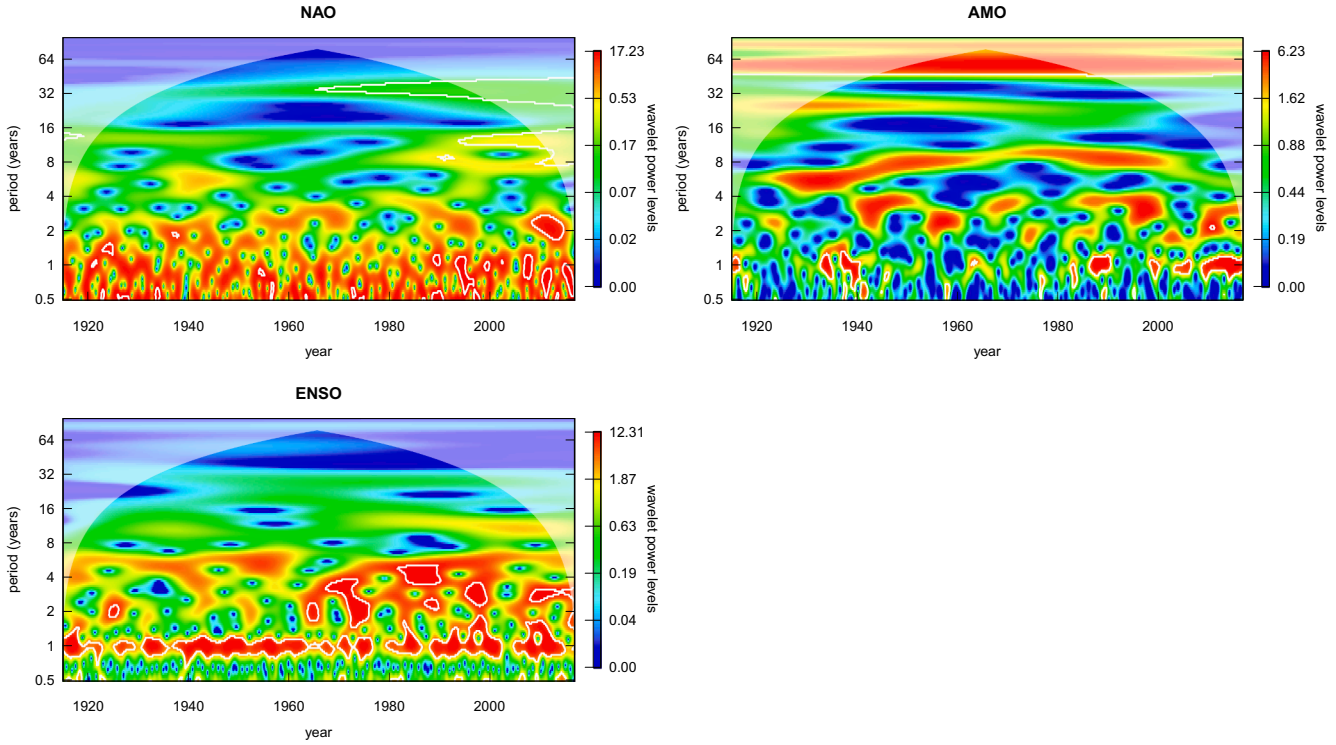

Fig. 3. Continuous wavelet power spectra of the regarded climate indices. Significant local maxima of the average power spectrum with average power and period are given in Table 2.

11 years, with 11.3 years being the global maximum, which shows a comparably low absolute average power of 3.957. This helps to support the findings that with increasing thickness of the unsaturated zone signals are damped and shorter periodic recharge signals are more sensitive to damping, though other factors controlling damping, like the mean annual infiltration flux, soil texture, or layering in the vadose zone, could not be evaluated due to lacking data. Nevertheless, this result fits well to the findings of Corona et al. (2018), who computed a damping depth of about 10–20 m for annual periods in a temperate climate.

In the Copenhagen and Tilburg wells, the one-year cycle is present, but not the global maximum. Copenhagen is a confined well, with a thick confining silt layer of 12.6 m. The maxima of the power spectrum are at 1 and 84.4 years, with the latter being second lowest of all global maximum by showing an average power of 2.838. The confining layer with its high thickness and rather low hydraulic conductivity might be an explanation of the overall damping of the signals as well as the lack of the shorter periodicities (beside the annual signal), assuming that the conductivity of the (semi-)confining layer is still high enough to conduct recharge signals. Another explanation could be damping of the recharge processes at the distant recharge areas of the aquifer. The power spectrum of the Copenhagen well also exhibits a change in behaviour from about 1970 on, where the significant periodicities, especially the one year cycle, seem to get vaguer, which may be due to an anthropogenic influence (pumping). The Tilburg well also shows rather low average power values, compared to the other unconfined wells in porous aquifers. Though a one year periodicity is present, its power is less than at 57.7 years, being the global maximum. This might be a result of the comparably fine material in contrast to the other unconfined wells in porous aquifers, which makes the shorter periodicities more prone to damping.

The other unconfined wells in porous aquifers have their global maxima of average power at one year, with values between 3.659 and 5.414. They also support the findings, that signals are damped with increasing depth to groundwater, since the average power of the one-year periodicity correlates well with decreasing depth to groundwater (Pearson $R = -0.97$, $p = 0.026$). Three of them also show significant local maxima at longer periodicities, namely at about 23 and 84 years, though with lower average powers.

Two wells show a very special behaviour: Chilgrove House and Dalton Home. Though they have rather thick unsaturated zones of (on average) 28 and 17 m, they show a decent one year periodicity with comparatively high average powers (10.086 and 7.730) as global maxima, which is about twice as much as for the other wells. This can be explained from the aquifer type, which is fractured to karstic. Due to low specific yields, the groundwater table reacts fast and damping is not as distinct as in porous aquifers. Among these two wells, Dalton Home, which is described as having a thin drift cover, shows more damping, which is also consistent with the earlier findings. The Chilgrove House well is the only one to show a periodicity of 6 months.

Concerning precipitation, all time series also show a one year cycle as the global maximum (significant maxima of the power spectra in Table 2, power spectra are provided as ESM). The average power values for the global maxima differ from 1.631 to 7.540, with a general trend to higher values with increasing continental climate. Most stations also show longer periodicities, but with overall low average powers (< 1.0).

For the NAO climate index, we found significant periodicities of half a year, about 13 and 33 years, with the global maximum at 6 months (Table 2). The principle periodicity of 8–9 years and a secondary periodicity of 3–5 years described in earlier works (Hurrell et al., 2003; Hurrell and Deser, 2009) are not classified as significant in the average power, but are at least partly visible in some time periods of the power spectrum (Fig. 3).

AMO shows three significant maxima of average power at 1.0, 57.7 and 84.4 years, with the global maximum at 57.7 years. A maximum at about 9 years, which is also mentioned in Barros et al. (2017), can be seen in the power spectrum, but is not classified as significant. The longer periodicities described by others (e.g. Barros et al., 2017, Wyatt et al., 2011) for AMO of 50–80 years can thereby be confirmed (Fig. 3).

ENSO shows the highest average powers of all three climate indices,

Table 3
Significant ($p < 0.05$) local maxima (global maxima in bold) of average cross wavelet coherence of groundwater level and precipitation, NAO, AMO and ENSO for the nine regarded groundwater wells.

Well name	Climate station	WTC groundwater-precipitation			WTC precipitation – NAO			WTC precipitation - AMO			WTC precipitation - ENSO
		Period (years)	Average Coherence	p-value	Period (years)	Average Coherence	p-value	Period (years)	Average Coherence	p-value	Period (years)
Chilgrove House	Oxford	0.5	0.441	< 0.001	1.1	0.415	0.002	**1.1**	**0.350**	**0.030**	0.5
		1.0	0.518	< 0.001	**4.7**	**0.604**	**0.044**				**1.0**
		2.1	0.734	< 0.001							
		3.6	0.728	< 0.001							
		6.5	0.849	< 0.001							
		10.9	0.772	0.005							
		14.9	0.745	0.043							
		53.8	**0.950**	**0.035**							
Dalton Home	Sheffield	0.5	0.363	< 0.001	**4.1**	**0.593**	**0.046**	**1.0**	**0.368**	**0.002**	**1.0**
		1.0	0.573	< 0.001							
		4.4	**0.853**	< **0.001**							
		5.7	0.845	< 0.001							
		9.5	0.744	0.009							
		13.9	0.840	0.004							
Eglfing	Munich	0.5	0.522	< 0.001	**1.0**	**0.440**	< **0.001**	0.5	0.260	0.040	**1.0**
		1.0	0.511	< 0.001				1.0	0.504	< 0.001	
		1.9	0.620	< 0.001				**2.1**	**0.526**	**0.010**	
		3.6	0.770	< 0.001							
		4.9	0.818	< 0.001							
		11.3	**0.914**	< **0.001**							
		21.9	0.872	0.006							
Friedrichsdorf	Steinhagen	0.5	0.625	< 0.001	**4.3**	**0.608**	**0.033**				0.5
		1.0	0.457	< 0.001							1.0
		2.2	0.798	< 0.001							**19.0**
		3.6	0.816	< 0.001							
		5.1	0.885	< 0.001							
		8.9	0.845	0.001							
		13.9	**0.906**	**0.001**							
		19.7	0.903	0.001							
Fuhrberg	Hannover	0.5	0.497	< 0.001				**1.0**	**0.364**	**0.008**	0.5
		1.0	0.485	< 0.001							1.0
		3.2	0.822	< 0.001							**17.1**
		4.6	0.823	< 0.001							
		13.5	0.852	0.002							
		24.3	**0.888**	**0.007**							
		30.1	0.877	0.034							
Copenhagen	Copenhagen	0.5	0.387	< 0.001	**4.6**	**0.615**	**0.032**	**1.1**	**0.412**	< **0.001**	0.5
		1.0	0.568	< 0.001							1.0
		1.9	0.682	< 0.001							2.4
		3.7	0.877	< 0.001							**29.9**
		7.7	0.779	< 0.001							
		13.9	0.857	0.001							
		29.9	**0.886**	**0.019**							
Kork	Karlsruhe	0.5	0.567	< 0.001	**14.4**	**0.772**	**0.022**	25.1	0.848	0.029	0.5
		5.3	0.857	< 0.001				**68.6**	**0.983**	**0.014**	1.0
		15.5	**0.899**	< **0.001**							**55.7**

(*continued on next page*)

Table 3 (*continued*)

Well name	Climate station	WTC groundwater-precipitation			WTC precipitation – NAO			WTC precipitation - AMO			WTC precipitation - ENSO
		Period (years)	Average Coherence	p-value	Period (years)	Average Coherence	p-value	Period (years)	Average Coherence	p-value	Period (years)
Otterwisch	Halle	0.5	0.269	0.015	1.0	0.357	0.004	**1.1**	**0.440**	< **0.001**	0.5
		1.0	0.534	< 0.001	**12.6**	**0.849**	**0.001**				**1.0**
		3.9	0.659	0.005							
		8.6	0.713	0.019							
		13.5	**0.851**	< **0.001**							
Tilburg	De Bilt	0.5	0.383	< 0.001				**1.0**	**0.380**	< **0.001**	0.5
		1.0	0.616	< 0.001							1.0
		1.8	0.556	0.001							**5.9**
		2.1	0.552	< 0.001							
		5.3	0.841	< 0.001							
		6.3	**0.847**	< **0.001**							

Well name	WTC precipitation - ENSO		WTC groundwater - NAO			WTC groundwater - AMO			WTC groundwater - ENSO		
	Average Coherence	p-value	Period (years)	Average Coherence	p-value	Period (years)	Average Coherence	p-value	Period (years)	Average Coherence	p-value
Chilgrove House	0.268	0.014	1.1	0.462	< 0.001	1.0	0.531	< 0.001	0.5	0.308	0.001
	0.441	< **0.001**	**14.4**	**0.767**	**0.023**	**14.9**	**0.782**	**0.019**	0.9	0.779	< 0.001
									30.9	**0.879**	**0.027**
Dalton Home	**0.457**	< **0.001**	**1.0**	**0.401**	< **0.001**	1.0	0.497	< 0.001	**0.9**	**0.762**	< **0.001**
						22.6	**0.845**	**0.018**			
Eglfing	**0.839**	< **0.001**				0.9	0.364	0.001	**0.9**	**0.454**	< **0.001**
						2.1	**0.493**	**0.044**			
Friedrichsdorf	0.304	0.001	**1.1**	**0.460**	< **0.001**	**1.0**	**0.507**	< **0.001**	0.5	0.259	0.041
	0.485	< 0.001							**0.9**	**0.788**	< **0.001**
	0.799	**0.027**							18.4	0.766	0.043

(*continued on next page*)

Table 3 (*continued*)

Well name	WTC precipitation - ENSO		WTC groundwater - NAO			WTC groundwater - AMO			WTC groundwater - ENSO		
	Average Coherence	p-value	Period (years)	Average Coherence	p-value	Period (years)	Average Coherence	p-value	Period (years)	Average Coherence	p-value
Fuhrberg	0.286	0.008	1.1	0.438	< 0.001	1.0	0.542	< 0.001	**0.9**	**0.817**	< **0.001**
	0.578	< 0.001	**13.5**	**0.727**	**0.046**				15.5	0.814	0.017
	0.792	**0.019**									
Copenhagen	0.275	0.008	1.1	0.393	< 0.001	**1.0**	**0.416**	< **0.001**	**0.9**	**0.694**	< **0.001**
	0.691	< 0.001	**4.0**	**0.591**	**0.044**				2.3	0.522	0.027
	0.538	0.011									
	0.880	**0.028**									
Kork	0.303	< 0.001	**1.1**	**0.395**	< **0.001**	**1.0**	**0.447**	< **0.001**	1.0	0.636	< 0.001
	0.505	< 0.001							**30.9**	**0.924**	**0.006**
	0.969	**0.018**									
Otterwisch	0.290	0.003	1.0	0.407	< 0.001	1.0	0.464	< 0.001	**0.9**	**0.720**	< **0.001**
	0.706	< **0.001**	**13.0**	**0.757**	**0.025**	3.7	0.595	0.037	4.1	0.608	0.039
						24.3	**0.838**	**0.027**			
Tilburg	0.283	0.003	1.1	0.486	< 0.001	1.0	0.531	< 0.001	0.9	0.803	< 0.001
	0.613	< 0.001	**4.3**	**0.612**	**0.024**	**52.0**	**0.954**	**0.029**	5.1	0.640	0.041
	0.641	**0.038**							**55.7**	**0.968**	**0.033**

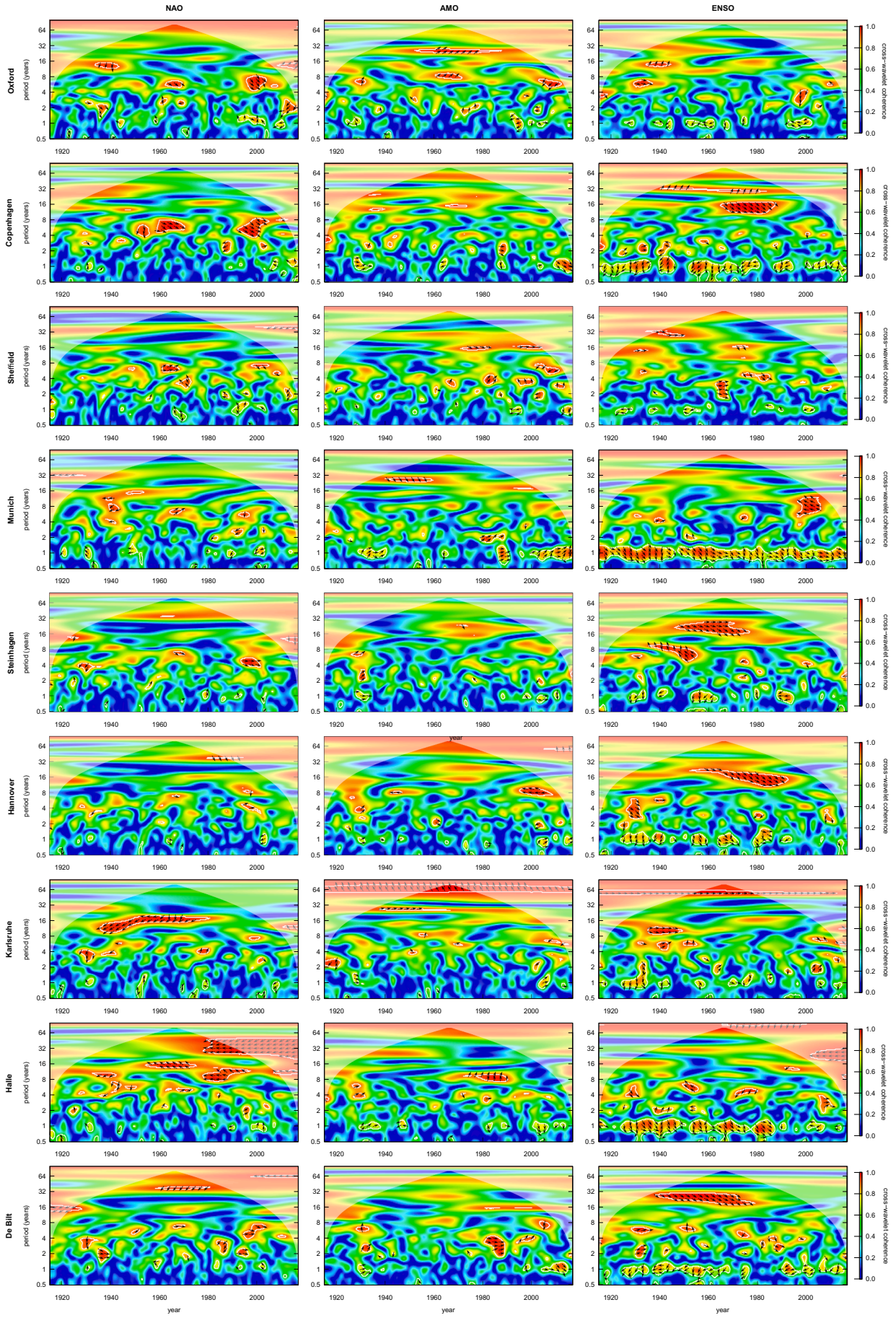

(caption on next page)

Fig. 4. Cross wavelet coherence of precipitation and NAO (left), AMO (middle) and ENSO (right) for the nine regarded climate stations. White lines indicate the 5% significance level. Parallel black arrows indicate coherence; arrows pointing exactly to the right indicate that the two series are in phase at the respective period, arrows pointing left indicate an opposite in phase behaviour.

with the global maximum at one year and secondary maximum with relatively high power at 2.5 years, becoming clearer from about the 1960s on, confirming the often described 2–7 years cycle. As NAO, ENSO also shows a maximum at 6 months, though the average power is not very high (Fig. 3).

3.2. Cross-wavelet analyses

3.2.1. Precipitation – climate indices

The cross-wavelet analyses of the precipitation time series of three of the considered climate stations and the NAO index show significant cross wavelet coherence at about one year, though with relatively low average coherence values of < 0.5, whereas six lack a common annual cycle (Table 3). Some of the stations also show significant coherences at periodicities of about 13–14 years (Karlsruhe, Halle) as well as of 30–40 years (Hannover, Halle, De Bilt, Table 3), especially from the 1960s on, though due to the long period the average coherence is in some cases not classified as significant (Fig. 4). Where significant, the 13–14 years cycles show relatively high average coherences of > 0.7. Some stations also reveal a coherent periodicity of about 4–5 years for some periods, which is most distinct for Sheffield, Steinhagen and Copenhagen, where it is significant on average over the whole time period. The stations of Steinhagen and Hannover are quite similar, which is not surprising as they are only about 100 km away from each other. The De Bilt and Hannover stations are the only ones without a significant average coherence with NAO, though the power spectra show significant coherences for parts of the time period (at about 14–16 years until 1930, about 32 years between 1960 and 1980, and around 64 years from 2000 on for De Bilt as well as about 32 years between 1980 and 2000 for Hannover). Regarding phase, the 13–14 years cycle is similar for the stations of Karlsruhe and Halle, with a phase difference of about a third to half a cycle duration. Though the influence of NAO on European climate, especially in winter precipitation, is widely recognized, it is overall rather complex (Wanner et al., 2001). While the influence is high in Northern Europe with a positive correlation between NAO and winter precipitation, and in Southern and Mediterranean Europe, with a strong negative correlation, it is low in the intermediate zone, where most of our assessed stations are situated, and diminishes eastward or with distance from the coastline (Rust et al., 2018). Furthermore, whilst the main atmospheric driver of winter precipitation variability is well established, that of summer precipitation remains unquantified due to the complexity of summer precipitation and diverse influencing factors involved (Tabari and Willems, 2018). Next to the contemporaneous relation between extreme precipitation and atmospheric circulation patterns, Tabari and Willems (2018) found that the long memory of atmospheric anomalies also creates a delayed influence, especially on extreme precipitation. The latter could possibly be an explanation of the phase difference of the found 13–14 year cycle, though in our results, the shift is slightly longer (5–6 years) than found by Tabari and Willems (2018). Regarding low-frequency variability, some studies suggest a nonstationary relationship of the NAO across Europe that is linked to interdecadal shifts in the location of the positions of the NAO pressure centers (Vicente-Serrano and López-Moreno, 2008; Moore et al., 2013). Such displacement of the pressure NAO centers points to possible existence of different NAO patterns, which could explain the lack of systematically strong correlations in the course of the twentieth century (Vicente-Serrano and López-Moreno, 2008), and has been particularly identified in the period of 1930–1950 and after the 1980s (Moore et al., 2013).

Though the overall coherence between precipitation and AMO is less distinct than for NAO, some stations also reveal coherences at longer cycles, at least for parts of the regarded time period, but again in most cases these are not classified as significant on average (Table 3), with the exception of the 25.1 years and 68.6 years cycles for Karlsruhe (average coherence of 0.848 and 0.983). Significant coherences in parts of the time period at about 8–16 years can be found for most stations, and at about 25 years for Oxford (between 1960 and 1980) and Munich (1940–1960). Most of the stations also suggest coherences at about 50–80 years, but only for Karlsruhe, this is significant, due to the long period, which is mostly covered by the cone of influence.

For ENSO there is a clear coherence maximum at the one-year cycle for all stations; seven out of nine stations show another local maximum for 6 months. Five stations show maxima at longer periods of about 2–7 years (Copenhagen, De Bilt), 17–19 years (Hannover and Steinhagen), 30 years (Copenhagen) and 56 years (Karlsruhe) on average. For Hannover, Steinhagen, Copenhagen and Karlsruhe, the maxima at 17, 19, 30 and 56 years, respectively, are the global maximum with average coherences of $\geq$ about 0.8. Overall, the coherences of a certain cycle only seem to be stable over shorter time periods of about 10–20 years. This is consistent with earlier findings of López-Parages and Rodríguez-Fonseca (2012), who have found a nonstationary strong and significant impact of ENSO on European rainfall in late winter just for those decades throughout the twentieth century in coincidence with negative phases of AMO.

Overall, precipitation and all three considered climate indices show significant coherences beyond the one-year cycle, at least for some of the regarded climate stations and parts of the time period, which supports earlier findings of an influence of NAO, AMO and ENSO on European climate.

3.2.2. Groundwater – precipitation

Cross-wavelet analyses of groundwater wells and precipitation of the respective climate station expectedly show significant coherence on a wide range of the power spectra with high average coherences of about 0.5 up to > 0.9 (Fig. 5 and Table 3), indicating that the groundwater level of the wells are influenced by the precipitation. Differences between confined and unconfined wells or different depths to groundwater regarding coherences of cycle lengths are not clearly obvious. All wells reveal coherences with precipitation for periods between six months and several years, three of them also for quite long cycles of 30 years (Fuhrberg-Hannover, Copenhagen) and 54 years (Chilgrove House-Oxford), but without a clear pattern. In terms of phase, the wells reveal clear differences for the one-year cycles. Most are out of phase, with different phase shifts between about a quarter of a cycle up to more than half a cycle (which could be three to more than six months, but also phase shifts of longer than one year are possible). For most of the wells, the phase shifts of the one-year cycle are varying over time. This can be explained by the fact that the propagation of the precipitation signal in the unsaturated zone, described by the Richards equation, is dependent on the prevailing moisture or water content, which is in turn dependent on the previous precipitation regime. This effect diminishes for longer periods and phase shifts are less likely to occur. Concerning the 2–8 year cycles, three of the unconfined wells in the porous aquifers (Fuhrberg, Kork, Otterwisch) as well as the unconfined Karstic Chilgrove House well show mostly in-phase coherences, indicating a probably direct reaction of the groundwater table to precipitation. The other unconfined wells in the porous aquifers show phase differences, depending on the cycle length. For Eglfing, this can be explained by lagging in consequence of the high depth to groundwater. For Tilburg and Friedrichsdorf, we can only speculate, that the lagging might be a result of a lower hydraulic conductivity (since no detailed information of the aquifers' hydraulic conductivities are

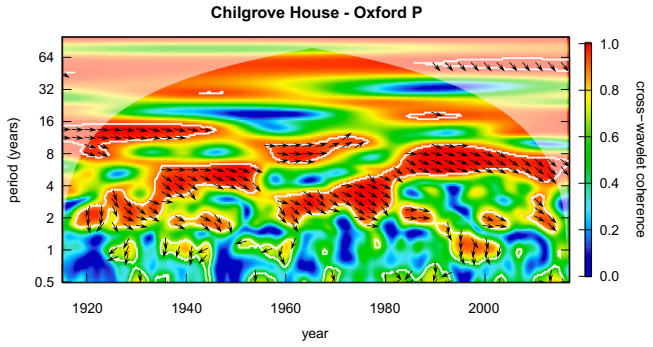

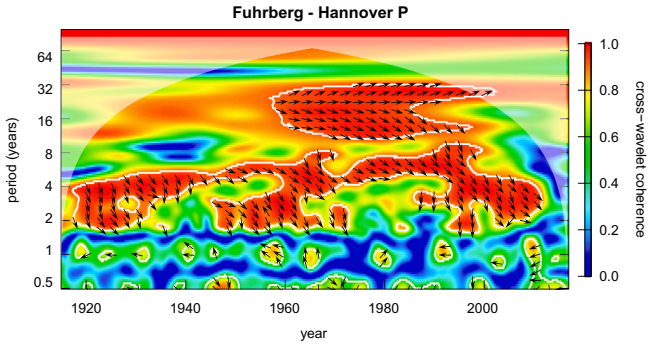

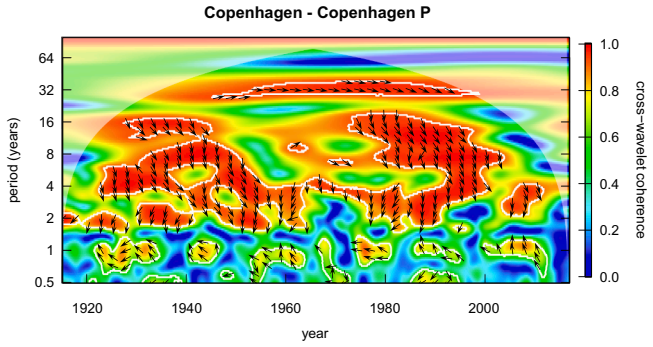

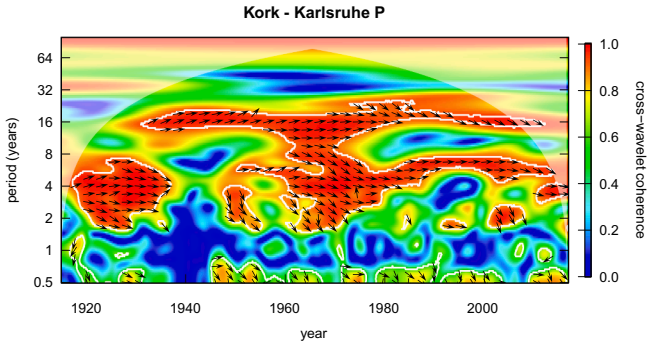

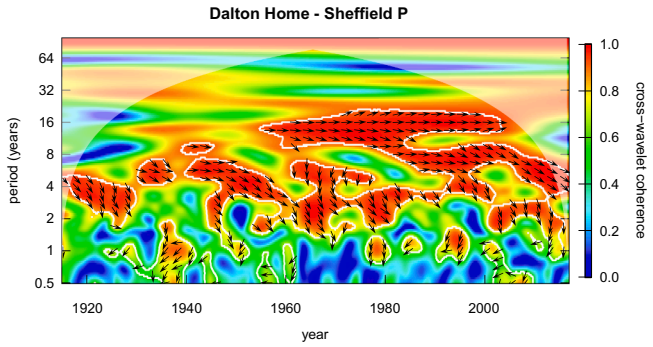

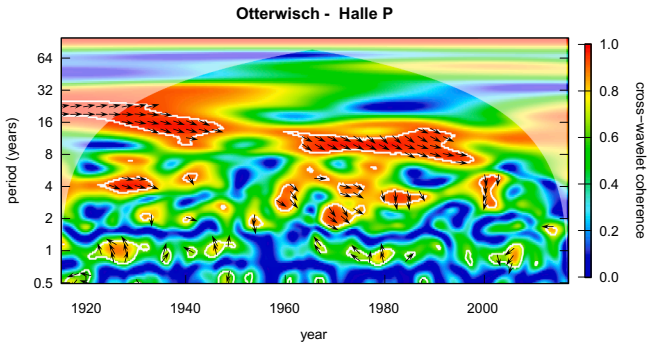

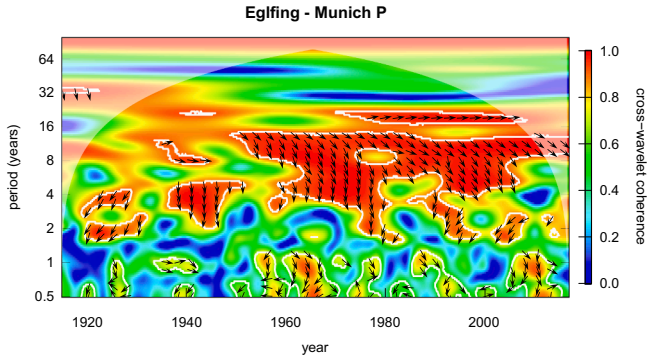

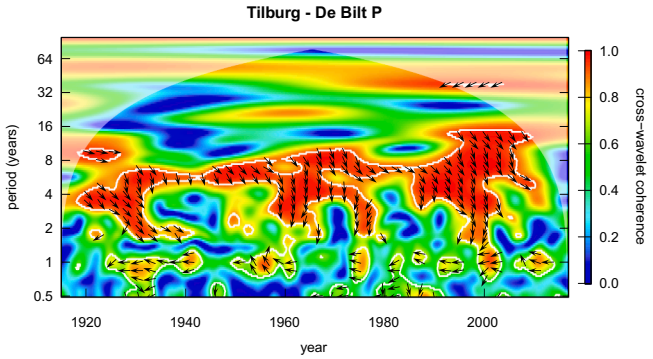

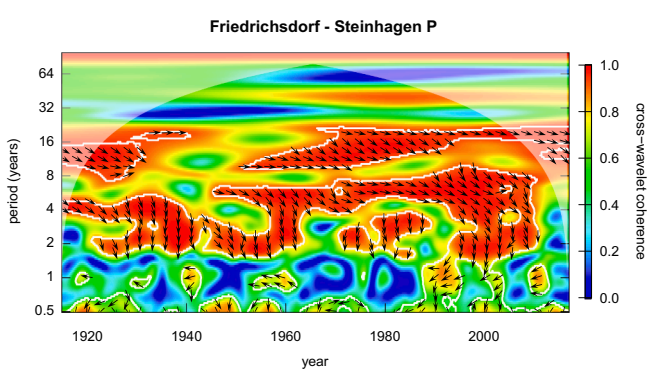

(caption on next page)

Fig. 5. Cross wavelet coherence of groundwater level and precipitation (P) for the groundwater wells and climate stations. White lines indicate the 5% significance level. Parallel black arrows indicate coherence; arrows pointing exactly to the right indicate that the two series are in phase at the respective period, arrows pointing left indicate an opposite in phase behaviour.

recorded). The confined/semi-confined wells (Copenhagen, Dalton Home) also show longer phase shifts, presumably as a result of retardation of the precipitation by the (semi-) confining layers. A damping of the signal for the (semi-)confined wells or higher depths to groundwater cannot directly be seen from the coherence analyses.

3.2.3. Groundwater – climate indices

Most of the groundwater wells show at least some time periods with significant coherence to all three climate indices (Fig. 6). Unlike for precipitation, the average coherences are higher for AMO than for NAO and highest for ENSO. For NAO, the coherence seems rather low on average, especially compared to precipitation (Table 3). Only the four more northern wells of Chilgrove House, Fuhrberg, Copenhagen and Tilburg show coherences at longer cycles of about 4 and 13–15 years respectively. This at least partly confirms earlier findings, that there is a stronger influence of NAO on the climate in Northern Europe, while in the intermediate zone, the correlation is overall low and diminishes eastward or with distance from the coastline (Rust et al., 2018).

Regarding AMO, four wells (Chilgrove House, Dalton Home, Otterwisch and Tilburg) show significant coherence at longer cycles of about 15, 23–25 and 52 years. Some of the wells, especially Eglfing and Tilburg, also suggest coherences at longer periods of about 60–80 years, though these are not classified as significant on average due to the long period.

ENSO shows the most distinct coherence of all climate indices to groundwater, with common cycles of one year for all wells, 2–5 years (Copenhagen, Otterwisch, Tilburg), 15–18 years (Fuhrberg, Friedrichsdorf), 31 years (Chilgrove House and Kork) up to 56 years (Tilburg).

For Eglfing, the overall coherence of groundwater and climate indices is rather low, which can again be explained by the thick unsaturated zone that leads to damping. An exception is the coherence to longer periods of AMO (at about 16–32 years from 1979 to 2000, and 64 years over the whole evaluated time span), though due to the long cycles, these are not classified as significant on average. Nevertheless, this is in accordance to the theory, that longer periods are less prone to damping.

3.2.4. Comparison of cross wavelet coherence of precipitation – climate indices and groundwater – climate indices

For most of the groundwater wells and precipitation series, the WTC power spectra with NAO, AMO and ENSO look somewhat similar. This might be expected, when assuming that the precipitation signal is propagated to groundwater. At a second look, interesting differences can be recognized. For some wells, like Chilgrove House, the coherences with the climate indices are more distinct for groundwater than for precipitation. This could be explained with the fact that the propagation of the precipitation to groundwater through the unsaturated zones acts like a noise filter. This can be seen for all cycle lengths, e.g. the one year cycle of ENSO (average coherence to groundwater 0.779 vs. average coherence to precipitation 0.441), or the 14.4 year cycle of NAO (average coherence to groundwater 0.767 vs. average coherence to precipitation 0.565) and 14.9 year cycle of AMO (average coherence to groundwater 0.782 vs. average coherence to precipitation 0.641) which are visible, but not as distinct, and both not classified as significant on average for precipitation. To a minor degree, this can also be observed for other wells. For Eglfing with its high depth to groundwater, the comparison shows that small periodicities, e.g. the one-year cycle visible in the WTC spectrum of precipitation and ENSO, are filtered out, whereas the longer periodicities (especially for AMO) are retained. The same can be seen for the Tilburg well, probably caused by a comparably low hydraulic conductivity of the unsaturated zone, and though not as distinct for Copenhagen and Dalton Home. For Fuhrberg and Otterwisch, the situation is not that clear. While the coherences for AMO and ENSO seem to be higher to groundwater, for NAO it is higher for precipitation, at least for cycles of more than one year.

4. Conclusions

We conducted wavelet analyses of nine groundwater level time-series in Europe with records of more than 100 years (from 1915 to 2016), and analysed possible impacts of precipitation and climatic teleconnections on long-term fluctuations of groundwater levels.

The major findings and conclusions can be summarized as follows:

- Univariate wavelet analyses of long-term groundwater level time-series show periodicities beyond the 1-year cycle, namely at about 2–7 years, 20–30 and 60–80 years, at least for some periods in the evaluated time span. Especially longer periods of 11, 23, 57.7 and 84.4 years are classified as significant, the two latter for several of the considered wells, though these are on the edge of significance due to the relatively short length of the recorded time span compared to the cycle duration.
- Our analyses provide additional support of previous findings, that with increasing thickness of the unsaturated zone, signals are damped and shorter periodic recharge signals are more sensitive to damping. Moreover, our results suggest that with lower permeability, especially the shorter signals get damped, whereas fractured to karstic aquifers with a lower specific yield are less prone to signal damping, in spite of high depths to groundwater.
- Cross-wavelet analyses of groundwater and precipitation show strong correlations over a wide range of periodicities, supporting the expected causal relation that climatic signals are propagated to groundwater levels via recharge. Here, the same findings for damping and lagging apply for the recharge signals.
- Our cross-wavelet analyses of precipitation at nine climate stations and the NAO, AMO and ENSO climate indices show significant correlations and coherences over the regarded periods, as previously suggested by some authors, indicating their influence on European climate.
- The periodic signals of NAO, AMO and ENSO propagate to groundwater via recharge, which could be shown by cross-wavelet analyses. All evaluated monitoring wells show significant relations in cross-wavelet power as well as cross-wavelet coherence to long-term climatic periodicities of NAO, AMO or ENSO. The average coherences are higher for AMO than for NAO and highest for ENSO, probably caused by the fact, that the majority of the considered wells is located in the intermediate zone, where the correlation of NAO and precipitation or groundwater, respectively, can be expected to be rather low. Major periodicities are 4 years and 13–14 years for NAO, about 15, 23–25, 52 and 60–80 years for AMO, and 2–5, 15–18, 31 and 56 years for ENSO. Some of the longer periodicities, especially for AMO, are on the edge of significance due to the relatively short length of the recorded time span compared to the cycle duration.

The shown periodic control on groundwater levels in Europe from the climate indices NAO, and especially AMO and ENSO offers a valuable source of longer term forecasting capability and should also be included or at least considered in analyses of anthropogenic trends and climate change effects, especially when regarding only shorter recorded groundwater time-series, which constitute the majority of available

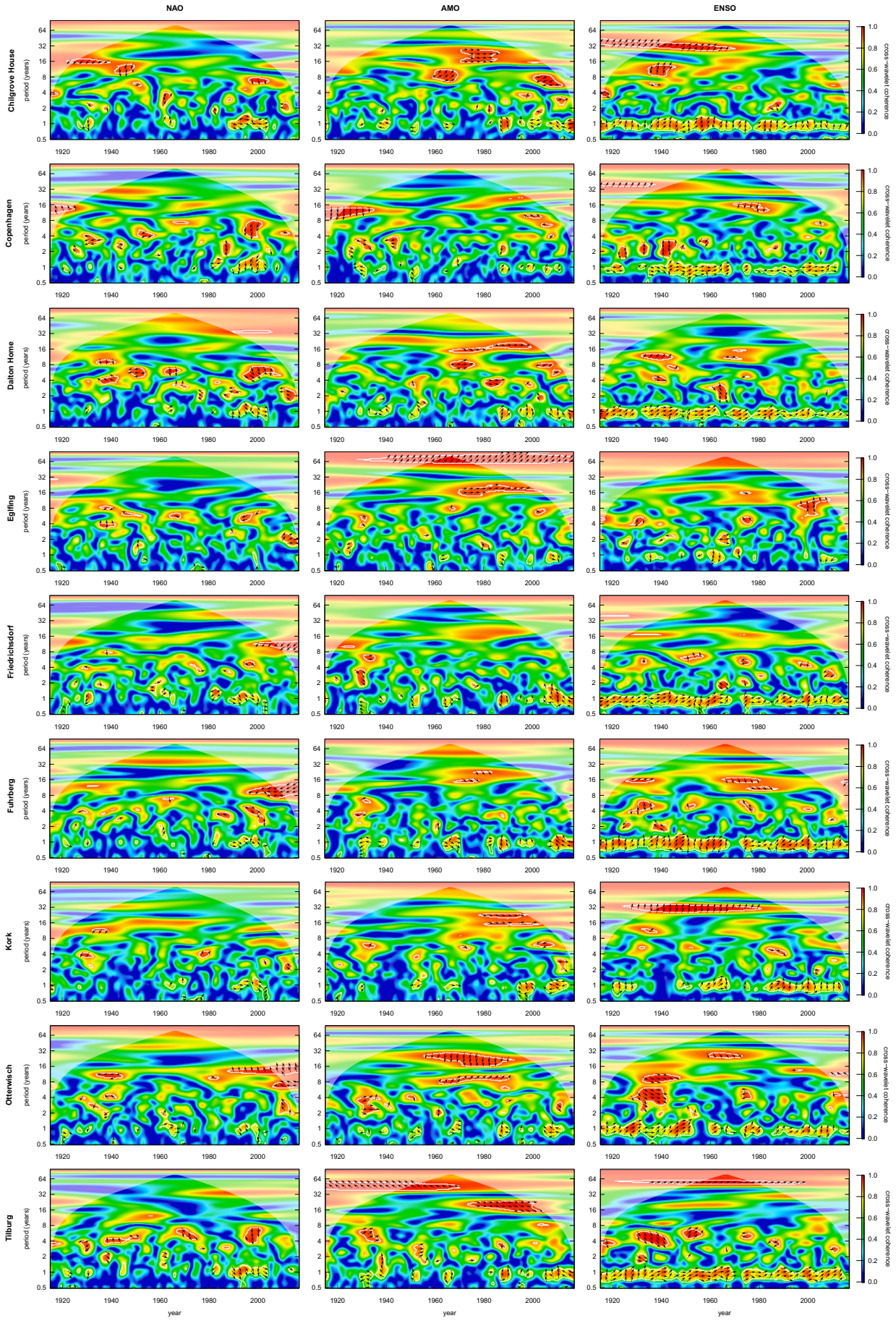

(caption on next page)

Fig. 6. Cross wavelet coherence of groundwater level and NAO, AMO and ENSO. White lines indicate the 5% significance level. Parallel black arrows indicate coherence; arrows pointing exactly to the right indicate that the two series are in phase at the respective period, arrows pointing left indicate an opposite in phase behaviour.

data. Moreover, our study shows the importance and value of long-term records of groundwater levels. This should be kept in mind, especially given the fact that during our search for long-term groundwater data, we found that in the last two decades, quite a few wells with previously long records were given up, probably as a result of cost savings.

Acknowledgements

Groundwater level data of the Chilgrove House and Dalton Home wells were kindly provided by the British Geological Survey. Groundwater level data of the remaining wells were taken from publicly available web services of the public authorities of Baden-Wurttemberg, Bavaria, Lower Saxony, North Rhine-Westphalia, Saxony, Denmark, and the Netherlands. We would also like to thank the three reviewers for their constructive comments.

Declaration of interest

None declared.

References

Alexander, M.A., et al., 2002. The atmospheric bridge: the influence of ENSO teleconnections on air-sea interaction over the global oceans. J. Clim. 15 (16), 2205–2231. https://doi.org/10.1175/1520-0442(2002) 015<2205:TABTIO>2.0.CO;2.

Anderson, W.P., Emanuel, R.E., 2008. Effect of interannual and interdecadal climate oscillations on groundwater in North Carolina. Geophys. Res. Lett. 35 (23). https://doi.org/10.1029/2008gl036054.

Bamston, A.G., Chelliah, M., Goldenberg, S.B., 1997. Documentation of a highly ENSO-related sst region in the equatorial pacific: Research note. Atmos. Ocean 35 (3), 367–383. https://doi.org/10.1080/07055900.1997.9649597.

Barros, A.P., Hodes, J.L., Arulraj, M., 2017. Decadal climate variability and the spatial organization of deep hydrological drought. 104005. Environ. Res. Lett. 12 (10). https://doi.org/10.1088/1748-9326/aa81de.

Bell, C.J., Gray, L.J., Charlton-Perez, A.J., Joshi, M.M., Scaife, A.A., 2009. Stratospheric communication of El Niño teleconnections to European winter. J. Clim. 22 (15), 4083–4096.

Bloomfield, J.P., Marchant, B.P., 2013. Analysis of groundwater drought building on the standardised precipitation index approach. Hydrol. Earth Syst. Sci. 17 (12), 4769–4787. https://doi.org/10.5194/hess-17-4769-2013.

Brönnimann, S., Xoplaki, E., Casty, C., Pauling, A., Luterbacher, J., 2007. ENSO influence on Europe during the last centuries. Clim. Dyn. 28 (2–3), 181–197. https://doi.org/10.1007/s00382-006-0175-z.

Charlier, J.-B., Ladouche, B., Maréchal, J.-C., 2015. Identifying the impact of climate and anthropic pressures on karst aquifers using wavelet analysis. J. Hydrol. 523, 610–623. https://doi.org/10.1016/j.jhydrol.2015.02.003.

Chaudhuri, A.H., Gangopadhyay, A., Bisagni, J.J., 2011. Response of the gulf stream transport to characteristic high and low phases of the North Atlantic Oscillation. Ocean Model. 39 (3–4), 220–232. https://doi.org/10.1016/j.ocemod.2011.04.005.

Chen, Z., Grasby, S.E., 2009. Impact of decadal and century-scale oscillations on hydro-climate trend analyses. J. Hydrol. 365 (1–2), 122–133. https://doi.org/10.1016/j.jhydrol.2008.11.031.

Corona, C.R., Gurdak, J.J., Dickinson, J.E., Ferré, T.P.A., Maurer, E.P., 2018. Climate variability and vadose zone controls on damping of transient recharge. J. Hydrol. 561, 1094–1104. https://doi.org/10.1016/j.jhydrol.2017.08.028.

Cox, W.D., Meng, L., Khedun, C.P., Nordfelt, A., Quiring, S.M., 2009. Discharge variability for an artesian spring of the Edwards Aquifer: Comal Springs (1933â-“2007). Int. J. Climatol. 29 (15), 2324–2336. https://doi.org/10.1002/joc.1871.

Dickinson, J.E., Ferré, T., Bakker, M., Crompton, B., 2014. A screening tool for delineating subregions of steady recharge within groundwater models. Vadose Zone J. 13 (6).

Dieppois, B., Durand, A., Fournier, M., Massei, N., 2013. Links between multidecadal and interdecadal climatic oscillations in the North Atlantic and regional climate variability of northern France and England since the 17th century. J. Geophys. Res.: Atmos. 118 (10), 4359–4372. https://doi.org/10.1002/jgrd.50392.

Domeisen, D.I., et al., 2015. Seasonal predictability over Europe arising from El Niño and stratospheric variability in the MPI-ESM seasonal prediction system. J. Clim. 28 (1), 256–271.

Dong, L., Shimada, J., Kagabu, M., Fu, C., 2015. Teleconnection and climatic oscillation in aquifer water level in Kumamoto plain, Japan. Hydrol. Process. 29 (7), 1687–1703. https://doi.org/10.1002/hyp.10291.

Enfield, D.B., Mestas-Nuñez, A.M., Trimble, P.J., 2001. The Atlantic multidecadal oscillation and its relation to rainfall and river flows in the continental U.S. Geophys. Res. Lett. 28 (10), 2077–2080. https://doi.org/10.1029/2000gl012745.

European Environment Agency (EEA) under the framework of the Copernicus programme, 2012. Corine Land Cover (CLC) 2012, Version 18.5.1.

Fendeková, M., Pekárová, P., Fendek, M., Pekár, J., Škoda, P., 2014. Global drivers effect in multi-annual variability of runoff. J. Hydrol. Hydromech. 62 (3). https://doi.org/10.2478/johh-2014-0027.

Fleming, S.W., Quilty, E.J., 2006. Aquifer responses to El Nino-Southern Oscillation, Southwest British Columbia. Ground Water 44 (4), 595–599. https://doi.org/10.1111/j.1745-6584.2006.00187.x.

Foufoula-Georgiou, E., Kumar, P., 1994. Wavelet analysis in geophysics: an introduction. In: Efi, F.-G., Praveen, K. (Eds.), Wavelet Analysis and Its Applications. Academic Press, pp. 1–43. https://doi.org/10.1016/B978-0-08-052087-2.50007-4.

Fraedrich, K., 1994. An ENSO impact on Europe? Tellus A 46 (4), 541–552. https://doi.org/10.1034/j.1600-0870.1994.00015.x.

Grinsted, A., Moore, J.C., Jevrejeva, S., 2004. Application of the cross wavelet transform and wavelet coherence to geophysical time series. Nonlin. Processes Geophys. 11 (5/6), 561–566. https://doi.org/10.5194/npg-11-561-2004.

Gurdak, J.J., et al., 2007. Climate variability controls on unsaturated water and chemical movement, high plains aquifer, USA. Vadose Zone J. 6 (3), 533–547. https://doi.org/10.2136/vzj2006.0087.

Hanson, R.T., Newhouse, M.W., Dettinger, M.D., 2004. A methodology to asess relations between climatic variability and variations in hydrologic time series in the southwestern United States. J. Hydrol. 287 (1–4), 252–269. https://doi.org/10.1016/j.jhydrol.2003.10.006.

Herceg-Bulić, I., Mezzina, B., Kucharski, F., Ruggieri, P., King, M.P., 2017. Wintertime ENSO influence on late spring European climate: the stratospheric response and the role of North Atlantic SST. Int. J. Climatol. 37 (S1), 87–108.

Holman, I.P., Rivas-Casado, M., Bloomfield, J.P., Gurdak, J.J., 2011. Identifying non-stationary groundwater level response to North Atlantic ocean-atmosphere teleconnection patterns using wavelet coherence. Hydrogeol. J. 19 (6), 1269–1278. https://doi.org/10.1007/s10040-011-0755-9.

Huo, X., et al., 2016. Application of wavelet coherence method to investigate karst spring discharge response to climate teleconnection patterns. JAWRA J. Am. Water Resour. Assoc. 52 (6), 1281–1296. https://doi.org/10.1111/1752-1688.12452.

Hurrell, J.W., 1995. Decadal trends in the north Atlantic oscillation: regional temperatures and precipitation. Science 269 (5224), 676–679. https://doi.org/10.1126/science.269.5224.676.

Hurrell, J.W., Deser, C., 2009. North Atlantic climate variability: The role of the North Atlantic Oscillation. J. Mar. Syst. 78 (1), 28–41. https://doi.org/10.1016/j.jmarsys.2008.11.026.

Hurrell, J.W., Kushnir, Y., Ottersen, G., Visbeck, M., 2003. An overview of the North Atlantic oscillation. The North Atlantic Oscillation: Climatic Significance and Environmental Impact 134, 1–35.

Ineson, S., Scaife, A.A., 2009. The role of the stratosphere in the European climate response to El Niño. Nat. Geosci. 2 (1), 32.

Ionita, M., 2009. Variability and potential predictability of Elbe river streamflow and their relationship to global teleconnection patterns. PhD Thesis, University of Bremen, Bremen, Germany.

Jackson, C.R., Bloomfield, J.P., Mackay, J.D., 2015. Evidence for changes in historic and future groundwater levels in the UK. Prog. Phys. Geogr. 39 (1), 49–67. https://doi.org/10.1177/0309133314550668.

Jones, P.D., Jonsson, T., Wheeler, D., 1997. Extension to the North Atlantic oscillation using early instrumental pressure observations from Gibraltar and south-west Iceland. Int. J. Climatol. 17 (13), 1433–1450. https://doi.org/10.1002/(SICI)1097-0088(19971115)17:13<1433::AID-JOC203>3.0.CO;2-P.

Knight, J.R., Folland, C.K., Scaife, A.A., 2006. Climate impacts of the Atlantic multidecadal oscillation. Geophys. Res. Lett. 33 (17). https://doi.org/10.1029/2006gl026242.

Kumar, M., Duffy, C.J., 2009. Detecting hydroclimatic change using spatio-temporal analysis of time series in Colorado River Basin. J. Hydrol. 374 (1–2), 1–15. https://doi.org/10.1016/j.jhydrol.2009.03.039.

Kumar, P., Foufoula-Georgiou, E., 1997. Wavelet analysis for geophysical applications. Rev. Geophys. 35 (4), 385–412. https://doi.org/10.1029/97rg00427.

Kuss, A.J.M., Gurdak, J.J., 2014. Groundwater level response in U.S. principal aquifers to ENSO, NAO, PDO, and AMO. J. Hydrol. 519, 1939–1952. https://doi.org/10.1016/j.jhydrol.2014.09.069.

Labat, D., 2005. Recent advances in wavelet analyses: Part 1. A review of concepts. J. Hydrol. 314 (1–4), 275–288. https://doi.org/10.1016/j.jhydrol.2005.04.003.

López-Parages, J., Rodríguez-Fonseca, B., 2012. Multidecadal modulation of El Niño influence on the Euro-Mediterranean rainfall. Geophys. Res. Lett. 39 (2).

Luque-Espinar, J.A., Chica-Olmo, M., Pardo-Igúzquiza, E., García-Soldado, M.J., 2008. Influence of climatological cycles on hydraulic heads across a Spanish aquifer. J. Hydrol. 354 (1–4), 33–52. https://doi.org/10.1016/j.jhydrol.2008.02.014.

Mackay, J.D., et al., 2015. Seasonal forecasting of groundwater levels in principal aquifers of the United Kingdom. J. Hydrol. 530, 815–828. https://doi.org/10.1016/j.jhydrol.2015.10.018.

Maraun, D., Kurths, J., 2004. Cross wavelet analysis: significance testing and pitfalls. Nonlinear Processes Geophys. 11 (4), 505–514.

Mariotti, A., Zeng, N., Lau, K.M., 2002. Euro-Mediterranean rainfall and ENSO—a seasonally varying relationship. Geophys. Res. Lett. 29 (12), 59-1-59-4.

Markovic, D., Koch, M., 2005. Wavelet and scaling analysis of monthly precipitation extremes in Germany in the 20th century: Interannual to interdecadal oscillations and the North Atlantic Oscillation influence. Water Resour. Res. 41 (9). https://doi.org/10.1029/2004wr003843.
Markovic, D., Koch, M., 2014. Long-term variations and temporal scaling of hydroclimatic time series with focus on the German part of the Elbe River Basin. Hydrol. Process. 28 (4), 2202–2211. https://doi.org/10.1002/hyp.9783.
Massei, N., et al., 2007. Investigating possible links between the North Atlantic Oscillation and rainfall variability in northwestern France over the past 35 years. J. Geophys. Res. 112 (D9). https://doi.org/10.1029/2005jd007000.
Massei, N., Fournier, M., 2012. Assessing the expression of large-scale climatic fluctuations in the hydrological variability of daily Seine river flow (France) between 1950 and 2008 using Hilbert-Huang Transform. J. Hydrol. 448–449, 119–128. https://doi.org/10.1016/j.jhydrol.2012.04.052.
McGregor, G., 2017. Hydroclimatology, modes of climatic variability and stream flow, lake and groundwater level variability. Prog. Phys. Geogr. 41 (4), 496–512. https://doi.org/10.1177/0309133317726537.
Moore, G., Renfrew, I.A., Pickart, R.S., 2013. Multidecadal mobility of the North Atlantic oscillation. J. Clim. 26 (8), 2453–2466.
Moron, V., Ward, M.N., 1998. ENSO teleconnections with climate variability in the European and African sectors. Weather 53 (9), 287–295. https://doi.org/10.1002/j.1477-8696.1998.tb06403.x.
Morris, B.L., et al., 2003. Groundwater and its Susceptibility to Degradation: A Global Assessment of the Problem and Options for Management, Nairobi, Kenya.
Niedzielski, T., 2011. Is there any teleconnection between surface hydrology in Poland and El Niño/Southern Oscillation? Pure Appl. Geophys. 168 (5), 871–886. https://doi.org/10.1007/s00024-010-0171-4.
Perez-Valdivia, C., Sauchyn, D., Vanstone, J., 2012. Groundwater levels and teleconnection patterns in the Canadian Prairies. Water Resour. Res. 48 (7). https://doi.org/10.1029/2011wr010930.
Pohlmann, H., Sienz, F., Latif, M., 2006. Influence of the multidecadal Atlantic meridional overturning circulation variability on European climate. J. Clim. 19 (23), 6062–6067. https://doi.org/10.1175/JCLI3941.1.
Core Team, R., 2017. R: A Language and Environment for Statistical Computing. R Foundation for Statistical Computing, Vienna, Austria.
Rayner, N.A., Parker, D.E., Horton, E.B., Folland, C.K., Alexander, L.V., Rowell, D.P., Kent, E.C., Kaplan, A., 2003. Global analyses of sea surface temperature, sea ice, and night marine air temperature since the late nineteenth century. J. Geophys. Res. 108 (D14). https://doi.org/10.1029/2002jd002670.
Roesch, A., Schmidbauer, H., 2014. WaveletComp: A guided tour through the R-package.
Rust, W., Holman, I., Corstanje, R., Bloomfield, J., Cuthbert, M., 2018. A conceptual model for climatic teleconnection signal control on groundwater variability in Europe. Earth Sci. Rev. 177, 164–174. https://doi.org/10.1016/j.earscirev.2017.09.017.
Sang, Y.-F., 2013. A review on the applications of wavelet transform in hydrology time series analysis. Atmos. Res. 122, 8–15. https://doi.org/10.1016/j.atmosres.2012.11.003.
Smerdon, B.D., 2017. A synopsis of climate change effects on groundwater recharge. J. Hydrol. 555, 125–128. https://doi.org/10.1016/j.jhydrol.2017.09.047.
Sutton, R.T., Hodson, D.L.R., 2005. Atlantic ocean forcing of north American and European summer climate. Science 309 (5731), 115.
Tabari, H., Willems, P., 2018. Lagged influence of Atlantic and Pacific climate patterns on European extreme precipitation. Sci. Rep. 8 (1), 5748.
Taylor, C.M., Alley, W.M., 2001. Ground-Water-Level Monitoring and the Importance of Long-Term Water-Level Data.
Torrence, C., Compo, G.P., 1998. A practical guide to wavelet analysis. Bull. Am. Meteorol. Soc. 79 (1), 61–78. https://doi.org/10.1175/1520-0477(1998)079<0061:apgtwa>2.0.co;2.
Tremblay, L., Larocque, M., Anctil, F., Rivard, C., 2011. Teleconnections and interannual variability in Canadian groundwater levels. J. Hydrol. 410 (3–4), 178–188. https://doi.org/10.1016/j.jhydrol.2011.09.013.
Trenberth, K.E., 1997. The Definition of El Niño. Bull. Am. Meteorol. Soc. 78 (12), 2771–2778. https://doi.org/10.1175/1520-0477(1997) 078<2771:tdoeno>2.0.co;2.
Van Loon, A.F., 2015. Hydrological drought explained. Wiley Interdisciplinary Reviews: Water 2 (4), 359–392. https://doi.org/10.1002/wat2.1085.
Velasco, E.M., Gurdak, J.J., Dickinson, J.E., Ferré, T.P.A., Corona, C.R., 2017. Interannual to multidecadal climate forcings on groundwater resources of the U.S. West Coast. J. Hydrol.: Reg. Stud. 11, 250–265. https://doi.org/10.1016/j.ejrh.2015.11.018.
Vicente-Serrano, S.M., López-Moreno, J.I., 2008. Nonstationary influence of the North Atlantic Oscillation on European precipitation. J. Geophys. Res.: Atmos. 113 (D20).
Wanner, H., et al., 2001. North Atlantic oscillation–concepts and studies. Surv. Geophys. 22 (4), 321–381.
Wyatt, M.G., Kravtsov, S., Tsonis, A.A., 2011. Atlantic multidecadal oscillation and northern hemisphere's climate variability. Clim. Dyn. 38 (5–6), 929–949. https://doi.org/10.1007/s00382-011-1071-8.